

## Coordination/Organometallic Polymers Based on Diphosphine and Diisocyanide Ligands

Pierre D. Harvey

Département de chimie, Université de Sherbrooke, Sherbrooke, PQ, Canada, J1K 2R1  
E-mail: pierre.harvey@usherbrooke.ca

**Summary:** This paper reviews various coordination/ organometallic polymers in which the metal atoms are incorporated in the backbone using diphosphine and diisocyanide ligands. Such ligands includes diphosphines of the type bis(diphenylphosphino)alkane where alkane is  $(\text{CH}_2)_m$  with  $m = 1, 3-6$ , bis(diphenylphosphino)acetylene (dpa), and bis(dimethyl-phosphino)methane (dmpm), and diisocyanides such as 1,8-diiso-cyano-*p*-menthane (dmb) and *p*-diisocyanotetramethylbenzene (ditmb). The metal fragments are monocations such as  $\text{Cu}^+$ ,  $\text{Ag}^+$ , and  $\text{Au}^+$ , dinuclear species such as  $\text{Pd}_2(\text{dmb})_2^{2+}$ ,  $\text{Pd}_2(\text{dppm})_2^{2+}$ ,  $\text{M}_2(\text{dmpm})_3^{2+}$  ( $\text{M} = \text{Cu}, \text{Ag}$ ), and clusters such as  $\text{M}_4(\text{dmb})_4^{2+}$  ( $\text{M} = \text{Pd}, \text{Pt}$ ).

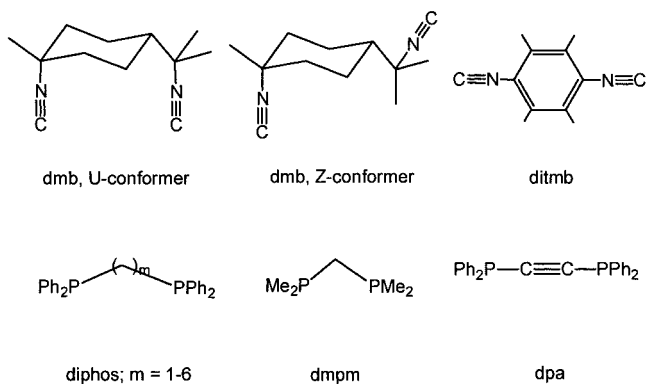
**Keywords:** bridging ligands; 1-D polymers; exciton; photoconductivity; photophysics

### Introduction

The syntheses and characterization of coordination and organometallic polymers in which the metal atoms are part of the macromolecule backbone, with the aim to prepare new materials finding applications in electric conductivity and photoconductivity, non-linear optical properties, sensors, liquid crystals, etc., is a still growing field. A number of challenges are associated with the fact that the fragments, or repetitive, units are held together by coordination bonds. The ligand lability directs the dissociation property of the polymer, causing two important problems. The first one is the addressibility of the structure in the solid state after dissolving the materials in different solvents or in the presence of different counter anions. Also depending on the ligand, some polymers can make rings, hence drastically changing the polymeric nature of the material. The second problem is that dissociation can be so extensive that the polymer is not present, or even oligomer in solution.

Over the years, this group has exploited two strategies to minimize the consequences of ligand lability. These are the use of two bridging ligands per metal fragment, and of more covalent M-L

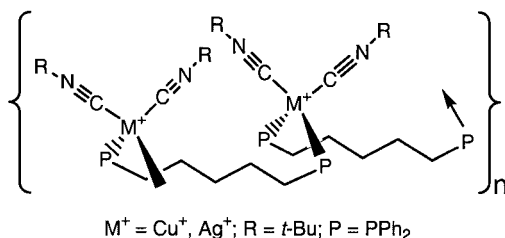
bondings. In the former case, the enhanced stability gained by the use of a second anchoring ligand reminds the gained stability with chelates. In the latter case, the electrostatic interactions supplementing those between soft metal cations and ligands contribute to render these ligands less labile. The danger is that if these M-L bonds are too "strong", then the polycationic polymers may become insoluble. This situation represents the other extreme. An undissociated and soluble polymers is the ideal case, but such a situation does not always occur. The intermediate scenario is when a polymer must partially dissociate in solution to form weakly soluble oligomers, which upon precipitation reform the original polymer. In this way, the polymer structure is still reproducibly addressable, and simple chemical transformation such as counter anion exchange can be performed without altering the polymeric nature of the materials. This paper describes the chemistry between various diphosphine and diisocyanide ligands,<sup>[1]</sup> with  $M^+$  ( $M = \text{Cu}, \text{Ag}, \text{Au}$ ),  $\text{Pd}_2^{2+}$ , and  $\text{M}_4^{2+}$  ( $M = \text{Pd}, \text{Pt}$ ) metallic fragments.



### Simple $\{\text{M}(\text{L-L})^{m+}\}_n$ Polymers

Using the diphosphines  $\text{Ph}_2\text{P}(\text{CH}_2)_m\text{PPh}_2$ , polymers of the type  $\{\text{M}(\text{Ph}_2\text{P}(\text{CH}_2)_m\text{PPh}_2)(\text{CN-}i\text{-Bu})_2^{2+}\}_n$  ( $M = \text{Ag}, \text{Cu}$ ;  $m = 4, 5$ ) have been prepared, some of which have been characterized from X-ray crystallography ( $M = \text{Ag}$  and  $M = \text{Cu}$ , the materials are amorphous). 1- and 2-D polymers have been observed. The replacement of  $\text{CN-}i\text{-Bu}$  by dmb leads to insoluble materials, presumably 3-D materials due to reticulation. These materials are found amorphous, and no glass

transition has been depicted between 0 and 200°C. However, computer modelling shows that the replacement of two adjacent CN-*t*-Bu ligands by one dmb does not perturb greatly the polymer chain, and the 1-D chain remains intact. The poor solubility may be then associated with a great molecular dimension of these materials.



The strongly luminescent and amorphous polymers of the type  $\{Au_2(dpa)(disphos)^{2+}\}_n$  (dipho =  $Ph_2P(CH_2)_mPPh_2$ ;  $m = 3\text{-}5$ , and  $Ph_2PCH_2CH(R)CH_2PPh_2$ ;  $R = O\text{-(CH}_2\text{)-O-naphthyl}$ ) have been prepared as well.<sup>[2]</sup> However, the mass spectra indicate ligand scrambling in the fragments, and the large FWHM (full-width-at-half-maximum) of the  $^{31}P$  NMR signal is consistent with the presence of chemical exchange in solution. The  $T_g$  observed in the differential scanning calorimetry traces (DSC), the emission lifetimes are function of the number of methylene fragments in the diphos ligand. Despite the scrambling of the ligands within the polymeric chain, these results indicate that it is still possible to control the thermal and photophysical properties of the materials. Table 1 summarizes the DSC data as examples. The photophysical data are presented below.

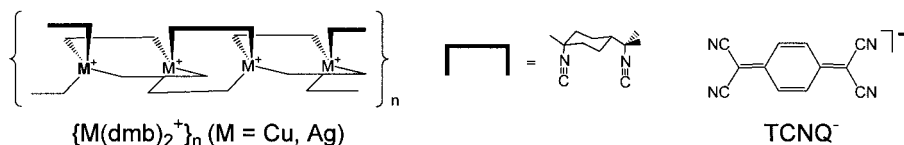
Table 1. DSC data of the  $\{Au_2(dpa)(disphos)^{2+}\}_n$  polymers

Polymers <sup>a</sup>	$T_g$	$\Delta C_p$
	$^{\circ}C$	$J/(g^{\circ}C)$
$\{Au_2(dpa)(Ph_2P(CH_2)_3PPh_2)^{2+}\}_n$	102.5	$0.07 \pm 0.01$
$\{Au_2(dpa)(Ph_2P(CH_2)_4PPh_2)^{2+}\}_n$	99.4	$0.08 \pm 0.01$
$\{Au_2(dpa)(Ph_2P(CH_2)_5PPh_2)^{2+}\}_n$	97.8	$0.10 \pm 0.01$
$\{Au_2(dpa)(Ph_2PCH_2CH(R)CH_2PPh_2)^{2+}\}_n$	83.6	$0.09 \pm 0.01$

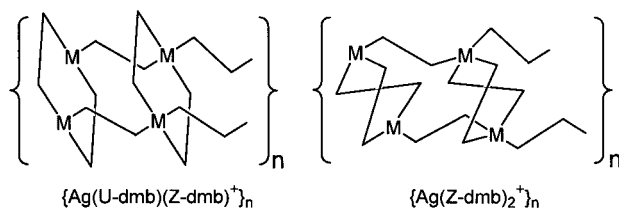
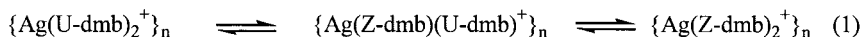
<sup>a</sup>  $R = O\text{-(CH}_2\text{)-O-naphthyl}$

## Polymers with Doubly Bridged Metal Atoms

The  $\text{Ag}^+$  and  $\text{Cu}^{2+}$  ions, and  $\text{Cu}(\text{NCMe})_4^+$  complex react with dmb in excess to form the corresponding 1-D polymer  $\{\text{M}(\text{dmb})_2^+\}_n$  where dmb is its U-shape, and the counter anions are  $\text{PF}_6^-$ ,  $\text{BF}_4^-$ ,  $\text{ClO}_4^-$ ,  $\text{NO}_3^-$ ,  $\text{CH}_3\text{CO}_2^-$  and  $\text{TCNQ}^-$  (tetracyanoquinodimethane anion).<sup>[3-5]</sup>



The structures reveal a  $\text{M}^{\text{III}}\text{M}$  separation and  $\text{M}_3$  angle of  $5\text{\AA}$  and  $140^\circ$ , respectively, in all cases. However, if the dmb is not in excess, the three latter counter anions lead to the formation of dimers,<sup>[6]</sup> while the three formers leads to dimers or trimers even in the excess of dmb.<sup>[7,8]</sup> Osmometry ( $M_n = 133000$ )<sup>[5]</sup> and light scattering ( $M_w = 155000$ )<sup>[4]</sup> establish the polymeric nature of  $\{\text{Cu}(\text{dmb})_2^+\}_n$ , while these techniques fail for  $\{\text{Ag}(\text{dmb})_2^+\}_n$  ( $M_n < 10000$ ).  $^{13}\text{C}$  NMR spin-lattice ( $T_1$ ) and NOE measurements (Nuclei Overhauser Enhancement) show that in fact the latter materials exist as oligomers in solution (7-8 units).<sup>[9]</sup> This property is due to the greater lability of the RNC ligand on  $\text{Ag}^+$ . This observation is further evidenced from the observation of the conformational isomers in the  $\{[\text{Ag}(\text{dmb})_2]\text{TCNQ}\}_n$  polymers, where dmb can be found in either the U- or Z-shape.<sup>[10]</sup> The polymeric isomers can be converted back and forth depending on the solvent used:

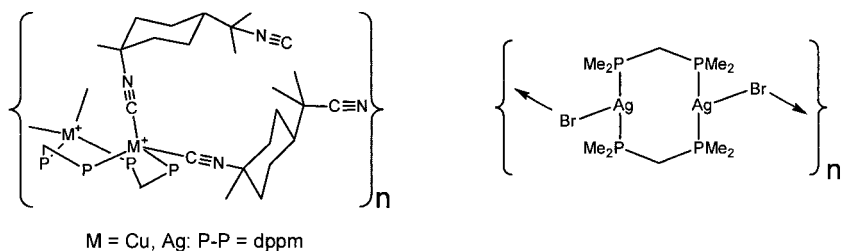


Control over the thermal properties for these materials can be achieved from the change of counter anion and doping agent such as in the  $\{[M(dmb)_2]TCNQ^xTCNQ^0\}_n$  polymers ( $M = Cu, Ag$ ;  $x = 1, 1.5$ ) as exemplified in Table 2. In these materials the glass transition is not associated with changes in chain conformation due to the rigidity of the polymer backbone.  $T_g$  is related to motion of the counter-ions, so that more free the counter-ion, lower  $T_g$  is.

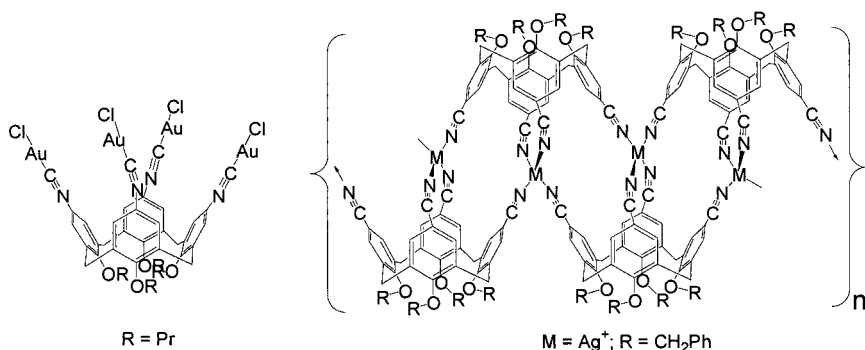
Table 2. DSC data for the  $\{[M(dmb)_2]TCNQ^xTCNQ^0\}_n$  polymers

Polymers	$T_g$	$\Delta C_p$	Morphology
	$^{\circ}C$	$J/(g^{\circ}C)$	
$\{[Ag(dmb)_2]TCNQ^{\cdot}CH_2Cl_2\}_n$	25.8	0.39	crystalline
$\{[Cu(dmb)_2]TCNQ^{\cdot}CH_2Cl_2\}_n$	25.0	0.37	semi-crystalline
$\{[Ag(dmb)_2]TCNQ^{\cdot}TCNQ^0\}_n$	37.7	0.19	highly crystalline
$\{[Cu(dmb)_2]TCNQ^{\cdot}TCNQ^0\}_n$	48.8	0.21	crystalline
$\{[Ag(dmb)_2]TCNQ^{1.5}TCNQ^0\}_n$	100.8	0.20	highly crystalline
$\{[Cu(dmb)_2]TCNQ^{1.5}TCNQ^0\}_n$	106.0	0.28	crystalline

Mixed-metal materials of the type  $\{Cu_{1-x}Ag_x(dmb)_2^+\}_n$  can also be prepared using a mixture of the starting materials in the desired ratio.<sup>[2]</sup> Such preparations lead to the control of the average size of the oligomers in solution, and the relative morphology. A systematic change in the unit cell parameters are noticed. The 1-D mixed-ligand polymers  $\{M(dmb)(dppm)^+\}_n$  ( $M = Cu, Ag$ ) have also been prepared as well.<sup>[2]</sup> Because of steric hindrance, the dmb ligand adopts the Z-conformation. These polymers are best described as polymers of  $M_2(dppm)_2^{2+}$  dimers ( $M = Cu, Ag$ ) bridged by two dmb's. The  $Ag^{\cdot} \cdots Ag^+$  separations are 4.4 and 11.5 Å for the dmpm- and dmb-bridged units, respectively.<sup>[2]</sup> Similarly to this example, the dimer  $Ag_2(dmpm)_2Br_2$  crystallizes to form a polymeric structure.<sup>[11]</sup> The  $Ag^{\cdot} \cdots Ag$  distances are 3.61 and 3.92 Å for the dmpm- and Br-bridged fragments, respectively. The dimers are weakly held together by longer Br-Ag bonds (2.95 Å), while the shorter bonds are 2.74 Å. The corresponding  $Au_2(dmpm)_2Cl_2$  dimer does not form a polymer, instead the complex behaves like a salt ( $[Au_2(dmpm)_2]Cl_2$ ). This behaviour is due to the poor tendency of the  $Au^+$  ion to form stable 4-coordinate complexes, while the 2-coordinate form is strongly favoured.



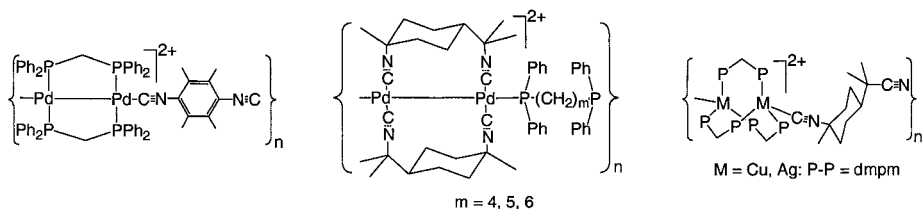
The ligand 5,11,17,23-tetrakisocyno-25,26,27,28-tetrapropoxycalix[4]arene (calix) can be used to coordinate  $\text{AuCl}$  fragments.<sup>[12, 13]</sup> The coordination of  $\text{Ag}^+$  produces a crystalline polymeric  $\{\text{M}(\text{calix})^+\}_n$  materials which is most likely related to the crystallographically characterized polymer  $\{5,11,17,23\text{-tetracyano-25,26,27,28-tetrabenzoxycalix[4]arenesilver(I)}\}_n$ .<sup>[14]</sup> Because of the tetradentate structure of the ligand, this 1-D material falls in this polymers with doubly bridged metal atom category. Contrarily to the corresponding  $\text{AuCl}$  complex, no luminescence in the solid state, nor in solution at 77K is depicted.



## Polymers of Dimers and Clusters

Numerous polymers can be prepared from axially functionalizable polynuclear complexes. Examples include dimers such as  $\text{Pd}_2(\text{dppm})_2^{2+}$ ,  $\text{Pd}_2(\text{dmb})_2^{2+}$  and  $\text{M}_2(\text{dmpm})_3^{2+}$  ( $M = \text{Cu}, \text{Ag}$ ), which are polymerized by one rigid, semi-rigid, and flexible bridging ligand such as ditmb, dmb, and diphosphines  $(\text{Ph}_2\text{P}(\text{CH}_2)_m\text{PPh}_2; m = 4-6)$ , respectively. Evidence for their polymeric structure in the solid state can be found in the thermal gravimetry analysis (TGA: large

temperature window of decomposition), DSC (presence of  $T_g$ ), X-ray powder diffraction pattern (XRD: presence of semi-crystalline or amorphous materials), and the fact that polymer film can easily be made. Using  $T_1$  measurements, these materials appear as oligomers in solution. For instance, the  $\{[\text{Pd}_2(\text{dmb})_2](\text{Ph}_2\text{P}(\text{CH}_2)_m\text{PPh}_2)^{2+}\}_n$  materials ( $m = 4-6$ ) exhibit only 3-4 units, which is a dimension similar to that of  $\{\text{Ag}(\text{dmb})_2^+\}_n$ .<sup>[9]</sup>



The polymers of clusters are also prepared from the axially functionalizable clusters, here the linear  $\text{M}_4(\text{dmb})_4^{2+}$ , using dmb ( $M = \text{Pd}$ )<sup>[15]</sup> and  $(\text{Ph}_2\text{P}(\text{CH}_2)_m\text{PPh}_2)$  ( $m = 4-6$ ).<sup>[16]</sup> The former has been characterized from X-ray crystallography, while the latter were characterized from the measurements of the intrinsic viscosity,  $[\eta]$ , and XRD; they were found to be amorphous polymers. It is believed that the limitation of the chain length is due to the presence of residual phosphine oxide and solubility. No glass transition was observed between 0 and 200°C. The  $\text{M}_4^{2+}$  fragment shows some sensitivity towards mild and unexpected oxidants, where  $\text{Pd}(\text{II})$ <sup>[13]</sup> and  $\text{Pt}(\text{I})$  species<sup>[15]</sup> have been observed as decomposition products.

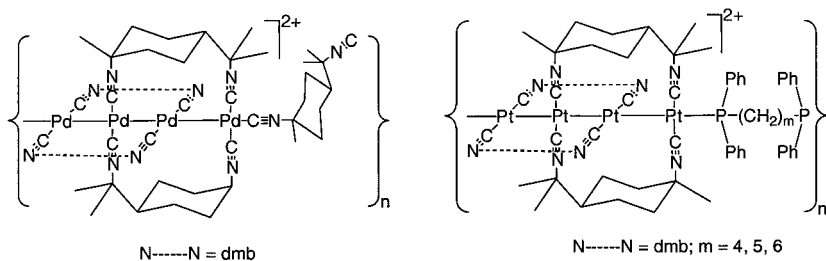


Table 3. Dimension of the  $\{\text{Pt}_4(\text{dmb})_4(\text{Ph}_2\text{P}(\text{CH}_2)_m\text{PPh}_2)\}_n$  polymers

Polymers	$[\eta]$	$M_n$	numbers of units
	$\frac{\text{cm}^3}{\text{g}}$		
$\{\text{Pt}_4(\text{dmb})_4(\text{Ph}_2\text{P}(\text{CH}_2)_4\text{PPh}_2)\}_n$	3.66	203000	100
$\{\text{Pt}_4(\text{dmb})_4(\text{Ph}_2\text{P}(\text{CH}_2)_5\text{PPh}_2)\}_n$	4.78	307000	150
$\{\text{Pt}_4(\text{dmb})_4(\text{Ph}_2\text{P}(\text{CH}_2)_6\text{PPh}_2)\}_n$	2.06	84000	40

### Semi- and Photoconductivity

The  $\{[\text{M}(\text{dmb})_2]\text{TCNQ}^x\text{TCNQ}^0\}_n$  polymers ( $x = 1, 1.5$ ) are semi-conductors with resistivities ( $\Omega$ ) for  $\text{M} = \text{Ag} \ll$  than  $\text{M} = \text{Cu}$ , consistent with the higher crystallinity of the Ag-materials.<sup>[5,18]</sup> The electric conductivity occurs through a mixed-valent  $\{\text{TCNQ}^{0.5-}\}_n$  or  $\{\text{TCNQ}^{0.4-}\}_n$  2-D layer (i.e. side-by-side chains placed in diagonal). An angle of about  $50^\circ$  is seen between the TCNQ-chain and polymer axes (Fig. 1). This result contrasts greatly with the generally encountered quasi-1-D  $\{\text{TCNQ}^x\}_n$  material where the counter ion is a simple alkalin or other simple cation, and where both cation and anion chains are placed parallel. This is due to the fact that the  $\text{M}^+$  ions are placed rigidly in the polymer structure at a distance that does not match the  $\pi$ -stacking distance of the TCNQ's. The observed resistivities (4-point probe technique on a pressed pellet) place the Ag-materials at the upper limit of the best semi-conducting materials. This performance is attributed to this 2D structure of the  $\{\text{TCNQ}^x\}_n$  layers.

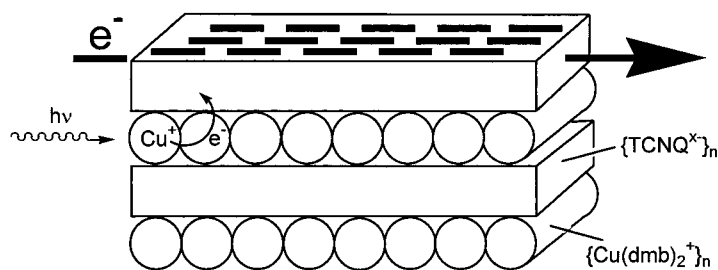


Figure 1. Scheme showing the layered structure of the  $\{[\text{M}(\text{dmb})_2]\text{TCNQ}^x\text{TCNQ}^0\}_n$  materials, and the mechanism for the photoconductivity. The fat bars represent up-right TCNQ chains.



The lesser conducting  $\{[M(dmb)_2]TCNQ^xTCNQ^0\}_n$  polymers ( $x = 1, 1.5$ ) are also photo-conducting. The current measured from the 4-point probe technique increases by 20% when a 200W lamp (broad band) is placed at 30cm in front of the pressed pellets. From various analyses of the photoreactions and photophysical processes using UV-vis and luminescence spectroscopy, it was possible to establish that the enhanced conductivity upon a water jacketed irradiation came from an electron transfer from the  $Cu(CNR)_4^+$  chromophore to the mixed-valent  $\{TCNQ^{\cdot-}\}_n$  layer.

## Luminescence Properties

The emission properties have been investigated in all cases in the solid state at room temperature. While most materials are weakly luminescent, the  $\{Au_2(dpa)(diphos)^{2+}\}_n$  and  $\{M_2(dmpm)_3(dmb)^{2+}\}_n$  polymers ( $M = Cu, Ag$ ) are strongly luminescent. Table 4 summarizes the emission data for these strongly luminescent materials. Similarly, the  $\{Pt_4(dmb)_4(Ph_2P(CH_2)_mPPh_2)\}_n$  polymers are luminescent, but somewhat less. At 77K, the intensity of luminescence increases. The  $[M_2(dmpm)_3(CN-*t*-Bu)_2]^{2+}$  and  $[Pt_4(dmb)_4(PPh_3)_2]^{2+}$  complexes are used as models for the building block of the corresponding polymers, and allow one to establish the effect of "polymerization" on the photophysical data. The key observations are that  $\tau_c$  for the non M-M bonded systems decreases as  $Cu > Ag > Au$ , consistent with the heavy atom effect on the phosphorescence due to the larger spin-orbital coupling constants. For the  $Pt_4$  systems, this heavy atom effect is more important as four heavy atom are connected together within the chromophore. The data also indicate that  $\tau_c$  is affected in the polymers. The expected decrease in  $\tau_c$  is associated with an increase in non-radiative pathways such as intramolecular vibrations (internal conversion into heat). In the  $Pt_4$  systems, the reverse case is observed because the replacement of the bulkier  $PPh_3$  ligands by the diphos  $Ph_2P(CH_2)_mPPh_2$  produces the reverse effect for the same reason.

Table 4. Photophysical data for some polymers

Materials <sup>a</sup>	$\lambda_{\text{max}}$	$\tau_c$	Conditions
	nm		
$[\text{Cu}_2(\text{dmpm})_3(\text{CN-}i\text{-Bu})_2]^{2+}$	477	$290 \pm 10 \text{ } \mu\text{s}$	room temp./solid
$\{\text{Cu}_2(\text{dmpm})_3(\text{dmb})^{2+}\}_n$	482	$259^b$	room temp./solid
$\{\text{Ag}_2(\text{dmpm})_3(\text{dmb})^{2+}\}_n$	448	$88^b$	room temp./solid
$\{\text{Au}_2(\text{dpa})(\text{Ph}_2\text{P}(\text{CH}_2)_3\text{PPh}_2)^{2+}\}_n$	495	$8.5 \pm 0.1 \text{ } \mu\text{s}$	room temp./solid
$\{\text{Au}_2(\text{dpa})(\text{Ph}_2\text{P}(\text{CH}_2)_4\text{PPh}_2)^{2+}\}_n$	495	$8.3 \pm 0.1 \text{ } \mu\text{s}$	room temp./solid
$\{\text{Au}_2(\text{dpa})(\text{Ph}_2\text{P}(\text{CH}_2)_5\text{PPh}_2)^{2+}\}_n$	495	$5.7 \pm 0.1 \text{ } \mu\text{s}$	room temp./solid
$\{\text{Au}_2(\text{dpa})(\text{Ph}_2\text{PCH}_2\text{CH}_2\text{CH}_2\text{PPh}_2)^{2+}\}_n$	none	-	room temp./solid
$[\text{Pt}_4(\text{dmb})_4(\text{PPh}_3)_2]^{2+}$	750	$2.71 \pm \text{ns}$	77K/EtOH
$\{\text{Pt}_4(\text{dmb})_4(\text{Ph}_2\text{P}(\text{CH}_2)_4\text{PPh}_2)\}_n$	736	$4.78 \pm \text{ns}$	77K/EtOH
$\{\text{Pt}_4(\text{dmb})_4(\text{Ph}_2\text{P}(\text{CH}_2)_5\text{PPh}_2)\}_n$	750	$5.15 \pm \text{ns}$	77K/EtOH
$\{\text{Pt}_4(\text{dmb})_4(\text{Ph}_2\text{P}(\text{CH}_2)_6\text{PPh}_2)\}_n$	755	$5.17 \pm \text{ns}$	77K/EtOH

<sup>a)</sup>  $\text{R} = \text{O}(\text{CH}_2)_6\text{O-naphthyl}$

<sup>b)</sup> The decays are polyexponential (see below), and only the maximum of the distribution is reported.

## Exciton Phenomena

For the polymers where weak emissions are observed at room temperature in the solid state, an unusual property is depicted. These weak emission are unusually broad and polarized, and exhibit non-exponential decays. Time-resolved emission spectroscopy shows that at short delays times, the emission bands are blue-shifted with respect to the maxima, and at longer ones, these are red-shifted. The progression of the shift from the blue to the red is continuous with delay times with no evidence for isosbestic points. These observations are diagnostic of an exciton phenomenon; an energy delocalization within the material. This delocalization can proceed in the bulk (intermolecular) or with the polymer itself (Fig. 2).

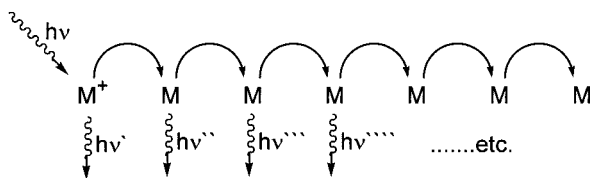
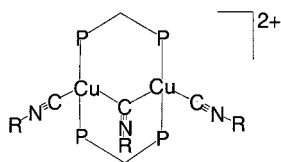


Figure 2. Scheme showing the exciton process.

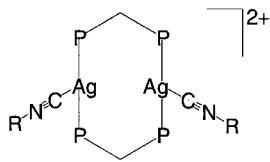
For instance, the  $\{M(\text{dmb})_2\}^+_n$  polymers ( $M = \text{Cu}, \text{Ag}$ ) exhibit emission decay traces that are non-exponential, but also are independent of the state of the materials (single crystal, powder, or in solution).<sup>[4]</sup> This important result indicates that energy transfer occur along the polymer chain through each  $M(\text{CN})_4^+$  chromophore. Interestingly, the emission lifetime and band position measured at the very early stage of the photophysical event are very similar to that of the corresponding isolated mononuclear complexes  $M(\text{CN-}t\text{-Bu})_4^+$  ( $M = \text{Cu}, \text{Ag}$ ). This means that the absorption is followed by an spontaneous emission from this same mononuclear chromophore, an event that occurs faster than the exciton process, but competes with the latter. It is possible to analyse the decay traces with a curve distribution. This distribution of lifetimes is characterized by maxima and width. More the exciton process is important, more the width is large, and more the emission band is large as well.

### Understanding the Synthons

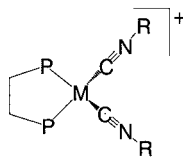
The reaction between  $\text{Cu}_2(\text{Ph}_2\text{P}(\text{CH}_2)_m\text{PPh}_2)_2(\text{NCMe})_4^{2+}$  ( $m = 4, 5$ ) with  $\text{CN-}t\text{-Bu}$  lead to colorless materials of the type  $\{\text{Cu}(\text{Ph}_2\text{P}(\text{CH}_2)_m\text{PPh}_2)(\text{CN-}t\text{-Bu})_2\}^{2+}_n$ . these amorphous materials swell when dissolved in various organic solvents and form thick solid film or wax. Parallely, the reaction between  $\text{Pd}(\text{Ph}_2\text{P}(\text{CH}_2)_m\text{PPh}_2)\text{Cl}_2$  ( $m = 3, 4$ ), or  $\text{Pd}_2(\text{Ph}_2\text{P}(\text{CH}_2)_m\text{PPh}_2)_2\text{Cl}_4$ , with  $\text{dmb}$  lead to completely insoluble colorless solids. The  $\text{Cu}^+$  and  $\text{Pd}^{2+}$  metal atoms coordinate 4 electron-donors in a tetrahedral and square planar fashion, respectively, and depending on the diphos used, monomer, dimer or polymer structures are observed  $\text{CN-}t\text{-Bu}$  and  $\text{dmb}$  complexes as shown in the next scheme.



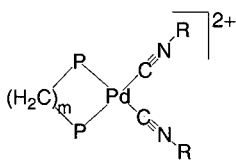
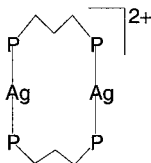
R = *t*-Bu



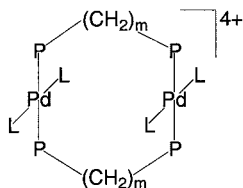
R = *t*-Bu



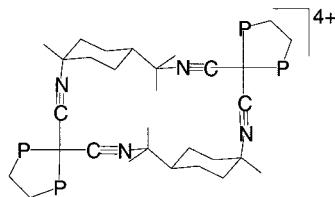
M = Cu, Ag; R = *t*-Bu



R = *t*-Bu; m = 2-4



L = CN-*t*-Bu; m = 5,6



While the dpmm ligand is largely (but not exclusively) an assembling ligand forming dimer species, the  $\text{Ph}_2\text{P}(\text{CH}_2)_m\text{PPh}_2$  ligands form a series of complexes where the structure varies gradually from mononuclear (chelate), to dimers (bridging), to polymers (bridging) with the increase in  $m$ . The dmb ligand (both U- and Z-forms) favours either dimers or polymers. Because of steric hindrance, longer methylene chains (avoiding chelate structures), and incompatibility of the bite distances, polymers are favoured with dmb/diphos-containing materials, as those described above. The "M(diphos)(CN-*t*-Bu)" structures summarized in the Scheme above reveal some clues about what is the metal environment for these amorphous or insoluble materials is.

## Acknowledgments

This research was supported by the NSERC (Natural Sciences and Engineering Research Council of Canada). PDH thanks the graduate students who did all the work; D. Perreault, D. Fortin, N. Jourdan, T. Zhang, M. Turcotte, F. Lebrun, E. Fournier, S. Sicard, P. Mongrain, and J.-F. Fortin.

- [1] P.D. Harvey, *Coord. Chem. Rev.* **2001**, 219, 17.
- [2] F. Lebrun, M.Sc. Dissertation, Université de Sherbrooke, **2001**.
- [3] D. Perreault, M. Drouin, A. Michel, P. D. Harvey, *Inorg. Chem.* **1992**, 31, 3688.
- [4] D. Fortin, M. Drouin, M. Turcotte, P. D. Harvey, *J. Am. Chem. Soc.* **1997**, 119, 531.
- [5] D. Fortin, M. Drouin and P.D. Harvey, *Inorg. Chem.* **2000**, 39, 2758.
- [6] D. Fortin, M. Drouin, P.D. Harvey, F.G. Herring, D.A. Summers, R.C. Thompson, *Inorg. Chem.* **1999**, 38, 1253.
- [7] P. D. Harvey, M. Drouin, A. Michel, D. Perreault, *J. Chem. Soc. Dalton Trans.* **1993**, 1365.
- [8] D. Perreault, M. Drouin, A. Michel, P.D. Harvey, *Inorg. Chem.* **1993**, 32, 1903.
- [9] M. Turcotte, P.D. Harvey, *Inorg. Chem.* **2002**, 41, 1739.
- [10] D. Fortin, M. Drouin, P.D. Harvey, *J. Am. Chem. Soc.* **1998**, 120, 5351.
- [11] D. Perreault, M. Drouin, A. Michel, V. M. Miskowski, W. P. Schaefer, P. D. Harvey, *Inorg. Chem.* **1992**, 31, 695.
- [12] J. Gagnon, M. Drouin, P.D. Harvey, *Inorg.Chem.* **2001**, 40, 6052.
- [13] P.D. Harvey, *Coord.Chem Reviews*, **2002**, 233-234, 289.
- [14] E. Elisabeth, L.J. Barbour, G.W. Orr, K.T. Holman, J.L. Atwood, *Supramol. Chem.* **2000**, 12, 317.
- [15] T. Zhang, M. Drouin, P.D. Harvey, *Inorg. Chem.* **1999**, 38, 1305.
- [16] T. Zhang, M. Drouin, P.D. Harvey, *Inorg. Chem.* **1999**, 38, 957.
- [17] T. Zhang, M. Drouin, P.D. Harvey, *Inorg. Chem.*, **1999**, 38, 4928.
- [18] D. Fortin and P.D. Harvey, *Coord. Chem. Rev.* **1998**, 171, 351.